The A-Star Puzzle
Proceedings IAU Symposium No. 224, 2004
J. Zverko, J. Žižňovský, S.J. Adelman, & W.W. Weiss, eds.

DOI: 10.1017/S174392130500952X

Diagnostics of λ Bootis stars' atmospheres using Na-D, Hα and Paschen lines

I. Kh. Iliev[1], I. Stateva[1], E. Paunzen[2] and I. Barzova[1]

[1]National Astronomical Observatory, Bulgarian Academy of Sciences,
P.O.Box 136, BG-4700 Smolyan, Bulgaria
e-mail: iliani@astro.bas.bg

[2]Astronomisches Institut der Universität Wien, A-1180 Wien, Austria

Abstract. High S/N high-resolution spectroscopic observations of seven bright well-known λ Bootis stars: HD 31295, HD 91130, HD 110411, HD 125162, HD 183324, HD 192640, and HD 221756 are presented. Sharp absorption details observed in the bottoms of the Na-D lines in HD 192640 and HD 221756 do not show any radial velocity changes with an accuracy up to 1 km s^{-1}. They are of interstellar origin. Manifestations of non-radial pulsation reported earlier in literature are observed both in the Na-D and the Hα line profiles. The Inglis-Teller formula was used to evaluate the electron density in the upper atmospheric layers ($\tau \sim 0.1$). The values obtained for log N_e are typical for normal A stars with similar effective temperatures and spectral classes.

Keywords. Techniques: spectroscopic, stars: atmospheres, stars: chemically peculiar, stars: individual (HD 31295, HD 91130, HD 110411, HD 125162, HD 183324, HD 192640, HD 221756)

1. Introduction

A small group named after the prototype λ Bootis is composed of Population I late-B to early-F stars with metal deficient atmospheres. The underabundances of Fe-peak elements reach up to 2 dex, while light elements such as C, N, O, and S are normal (solar). As a group λ Bootis stars occupy almost the same place in the H-R diagram as the Am stars and the cool Ap stars, which, in contrast, exhibit metal-enriched spectra. Many other types of stars can be found in this crowded area of the diagram including BHB, HAEBE, F-weak, field blue strugglers, intermediate Poplulation II, pre-MS, and δ Scuti stars. A small piece of the puzzle is presented in Table 1.

Table 1. Main stellar characteristics

	rotation	metals	magnetic field	variability
Normal A-stars	normal	normal	no	no, puls
Cool Ap-stars	slow	excess	yes	sp., ph., puls
Am-stars	slow	excess	no	no, puls?
λ Bootis	normal	deficit	no	no, puls

Our recent results (Iliev *et al.* 2002, Paunzen *et al.* 2002) show that the λ Bootis phenomenon occurs under very limited physical conditions, a fact that puts strong constrains on any theoretical model. Some of the leading concepts (Venn & Lambert 1992, Kamp & Paunzen 2002) postulate the crucial role of gas and dust around λ Bootis stars. Interaction with the circumstellar medium is considered to be the main reason that controls the observed peculiarities. Thus we began a project to observe the Na-D, the Hα, and the

Paschen lines as markers of the atmospheric structure, and indicators of possible ongoing interactions with the matter that surrounds each star.

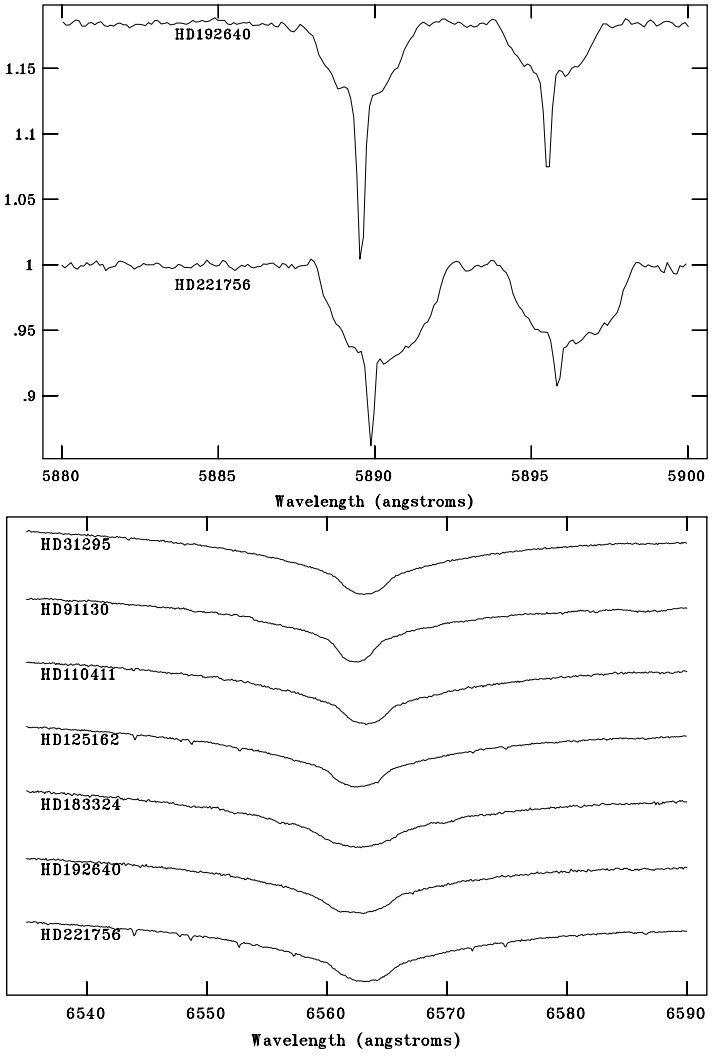

Figure 1. *Upper panel*: Na-D lines in the spectrum of HD 192640 and HD 221756. The upper spectrum is shifted by 0.2 for convenience. *Lower panel*: Hα cores. Small bumps are in the spectra of HD 91130, HD 125162, and HD 192640.

2. The observations

The spectroscopic observations were made with the 2-m RCC telescope of the Bulgarian National Astronomical Observatory Rozhen. Seven bright well-known and well-studied λ Bootis stars HD 31295, HD 91130, HD 110411, HD 125162, HD 183324, HD 192640, and HD 221756 have been observed in two spectral regions centered on the Na-D and the Hα lines as well as two regions near the Paschen jump including the interval between the Pa_{13} and the Pa_{21} lines. The resolving power R is about 30000. The typical S/N ratio

https://doi.org/10.1017/S174392130500952X Published online by Cambridge University Press

is about 300. Standard IRAF procedures were used for bias subtraction, flat-fielding and wavelength calibration. Hot, fast rotating stars were used for telluric lines removal.

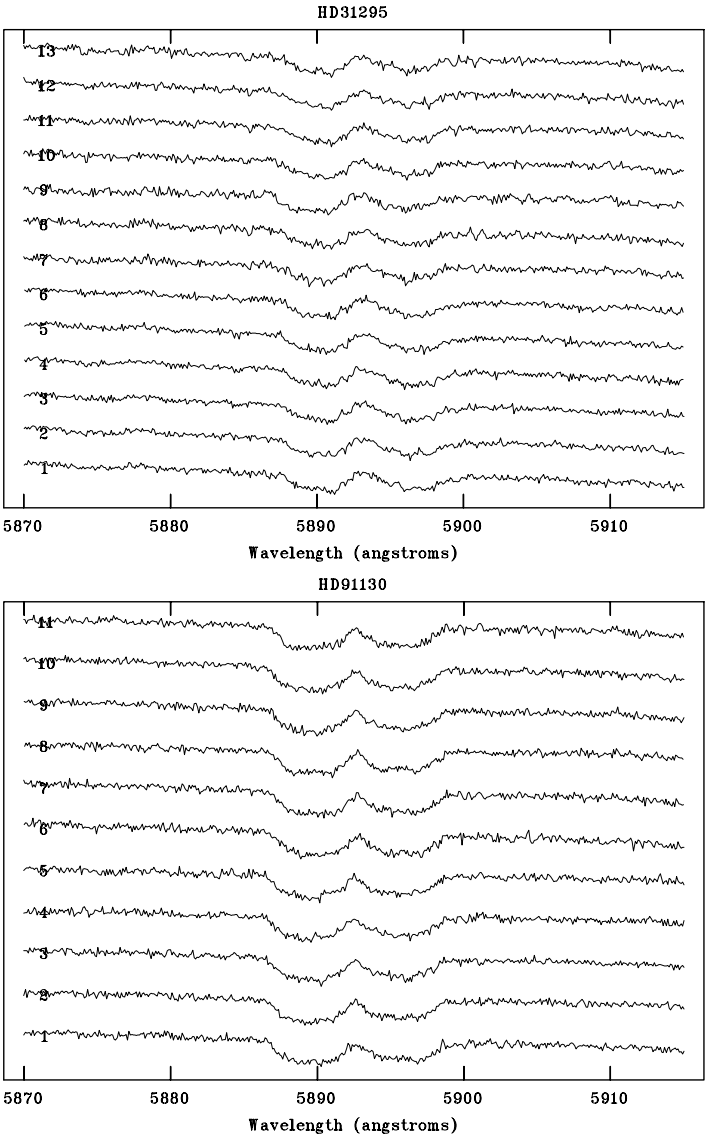

Figure 2. Na-D lines: time variation series for HD 31295 (top) and for HD 91130 (bottom).

3. Results

3.1. *Sharp Na-D details and Hα*

Sharp Na-D and Hα details are inherent in two of our stars : HD 192640 and HD 221756. They have been observed in the line bottoms and have a constant radial velocity: $-19.8\pm$ 1.2 km s^{-1} in HD 192640 (7 measurements, over a time span of about two months), and -3.7 ± 1.5 km s^{-1} in HD 221756 (3 measurements over the same time span). Note that

https://doi.org/10.1017/S174392130500952X Published online by Cambridge University Press

the case of HD 221756 is asymmetrical (see Fig. 1, upper panel). Sharp absorption details have an interstellar origin.

The rotational cores of the Hα lines are smooth and free of weak emissions. Some deviations from the regular (rotational broadened) shape in the spectra of HD 91130, HD 125162, and especially HD 192640 can be seen (Fig. 1, lower panel).

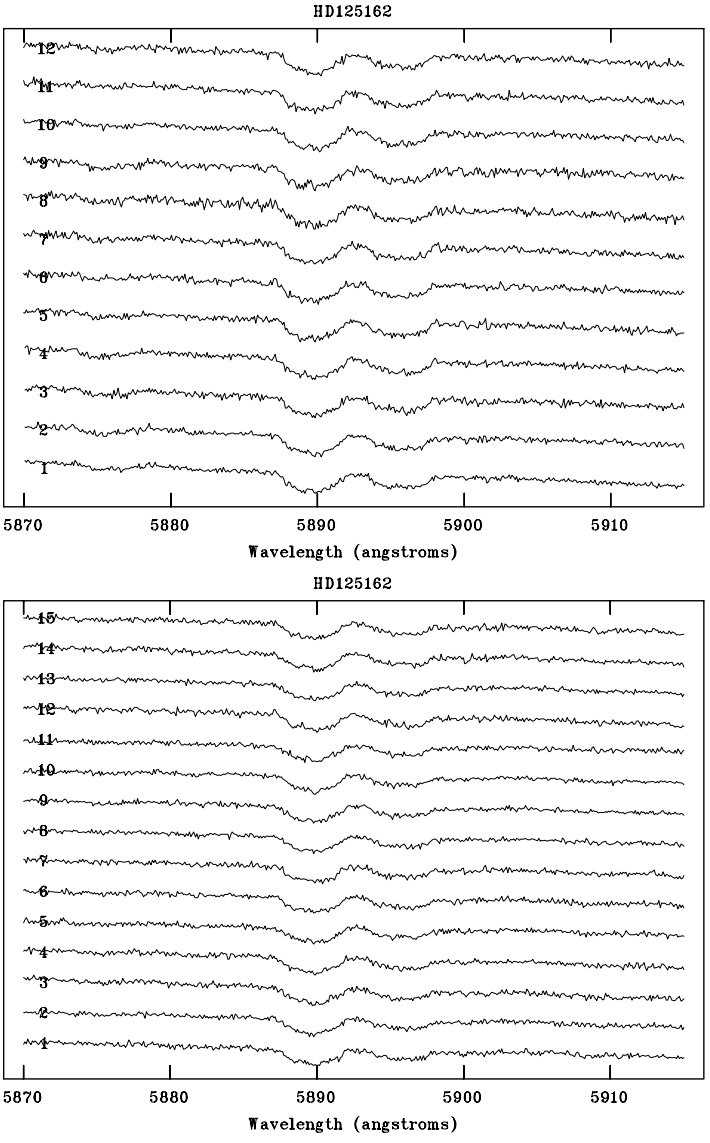

Figure 3. Na-D lines: time variation series for HD 125182.

3.2. *Non-radial pulsations*

Time dependent distortions from the regular shape observed previously by Bohlender *et al.* (1999) are seen in the Na-D line profiles. The short time scale evolution of these profiles is shown in the Fig. 2 upper panel: HD 31295 - two sequences consisting of spectra

https://doi.org/10.1017/S174392130500952X Published online by Cambridge University Press

numbered 1-6, and 7-13, each sequence lasts 60 minutes; lower panel: HD 91130 - two sequences consisting of spectra numbered 1-5, and 6-11, 60 minutes for each sequence. The star HD 125162 is persented in Fig. 3 with two sequences. They are numbered 1-15 and 1-12, both are 75 minutes long. The most prominent "complex" or even "flat bottom" cases are: HD 31295 with spectra 2, 10, and 12; HD 91130 with spectra 2, 4, 7, 8, and 11; HD 125162 with spectra 2 and 14 (upper panel), and with spectra 6, 7, 12, and 14 (lower panel).

3.3. *Electron density* $N_{\rm e}$

The Inglis-Teller formula connects the electron density $N_{\rm e}$ with the number of the last resolved hydrogen line (Balmer in the visible region and/or Paschen in the near infrared): $\log N_{\rm e} = 22.7 - 7.5 \log n_{\rm max}$. Thus we can estimate how dense are the uppermost atmospheric layers where the optical depth τ is close to 0.1. Typical values of $n_{\rm max}$ are shown in Table 2.

Table 2. Last resolved hydrogen-line number $n_{\rm max}$

A0–F0	ZAMS	mid-MS	TAMS	sub-giant
$n_{\rm max}$	17	18.5	20	21

n_{max} is determined when the Paschen lines vanish (their central depths $R_{\rm c}$ or equivalent widths W approach zero). Corrections are made to account for the overlapping of the line wings mainly due to rotation. Typical errors in $n_{\rm max}$ are about 0.2 - 0.25.

Table 3 contains our final results. The range of $\rm N_e$ values is typical for main sequence stars. However, at least three stars: HD 31295, HD 192640, and HD 221756 show $n_{\rm max}$ values a bit larger than expected from their positions inside the main sequence strip. The most plausible explanation points to extended or "giant-like" atmospheres.

Table 3. Electron densities

HD	$T_{\rm eff}$	$\log g$	$v \sin i$	$n_{\rm max}$	$\log N_{\rm e}$
31295	8920	4.20	123	20.0	13.24
91130	8135	3.78	152	19.9	13.25
110411	8970	4.36	154	19.8	13.28
125162	8720	4.07	115	17.8	13.63
183324	8950	4.13	100	17.5	13.67
192640	7940	3.95	80	21.1	13.08
221756	8510	3.90	105	20.5	13.17

Acknowledgements

II and IS gratefully acknowledge the support provided by the SOC and the LOC of the Symposium.

References

Bohlender, D.A., Gonzalez, J.-F. & Matthews, J.M. 1999, *A&A* 350, 553

Iliev, I.Kh., Paunzen, E., Barzova, I.S., Kamp, I., Griffin, R., Claret, A. & Koen, C. 2002, *A&A* 381, 914

Kamp, I. & Paunzen, E. 2002, *MNRAS* 335, L45

Paunzen, E., Iliev, I.Kh., Kamp, I. & Barzova, I.S. 2002, *MNRAS* 336, 1030

Venn, K.A. & Lambert, D.A. 1992, *ApJ* 363, 234